

# Measuring the Mean Lifetime of Cosmic Muons

Jason R. Heimann  
and  
John Wray

October 25, 2004

# Contents

|          |                                       |          |
|----------|---------------------------------------|----------|
| <b>1</b> | <b>Introduction</b>                   | <b>1</b> |
| <b>2</b> | <b>Experimental Apparatus</b>         | <b>1</b> |
| 2.1      | Absorber . . . . .                    | 1        |
| 2.2      | Counters . . . . .                    | 2        |
| 2.3      | Electronic modules . . . . .          | 2        |
| 2.3.1    | Discriminator . . . . .               | 3        |
| 2.3.2    | Logic . . . . .                       | 3        |
| 2.3.3    | Gate generator . . . . .              | 3        |
| 2.3.4    | Time to amplitude converter . . . . . | 4        |
| 2.4      | Data acquisition system . . . . .     | 4        |
| 2.5      | Other equipment . . . . .             | 4        |
| <b>3</b> | <b>Procedure</b>                      | <b>4</b> |
| 3.1      | Calibration . . . . .                 | 5        |
| 3.2      | Counter characterization . . . . .    | 5        |
| 3.3      | Logic setup . . . . .                 | 6        |
| 3.4      | Measurement . . . . .                 | 6        |
| <b>4</b> | <b>Results</b>                        | <b>6</b> |
| 4.1      | Calibration . . . . .                 | 6        |
| 4.2      | Counter characterization . . . . .    | 6        |
| 4.3      | Measurement . . . . .                 | 7        |
| <b>5</b> | <b>Analysis and Interpretation</b>    | <b>7</b> |
| 5.1      | Theory . . . . .                      | 7        |
| 5.2      | Experiment . . . . .                  | 7        |
| <b>6</b> | <b>Conclusion</b>                     | <b>8</b> |
| <b>7</b> | <b>Tables and Figures</b>             | <b>8</b> |

## List of Tables

|    |   |    |
|----|---|----|
| 1  | Results of TAC / MCA calibration . . . . .                                  | 8  |
| 2  | Details of linear fit . . . . .   | 8  |
| 3  | Results of 100 sec. of measurement with PMT A at three thresholds . . . . . | 11 |
| 4  | Results of 100 sec. of measurement with PMT B at three thresholds . . . . . | 12 |
| 5  | Results of 100 sec. of measurement with PMT C at three thresholds . . . . . | 13 |
| 6  | Results of 100 sec. of measurement with PMT D at three thresholds . . . . . | 14 |
| 7  | Efficiency measurements for counter A . . . . .                             | 17 |
| 8  | Efficiency measurements for counter B . . . . .                             | 17 |
| 9  | Efficiency measurements for counter C . . . . .                             | 18 |
| 10 | Efficiency measurements for counter D . . . . .                             | 18 |

|    |   |    |
|----|---|----|
| 11 | Operating parameters for counters . . . . .                             | 18 |
| 12 | Coincidence rates from counters in experimental configuration . . . . . | 18 |
| 13 | Re-binned results of experiment . . . . .                               | 21 |
| 14 | Details of curve fit . . . . .  | 21 |

## List of Figures

|    |   |    |
|----|---|----|
| 1  | The distribution of electron kinetic energies in muon decay at rest. Data from the experiment of Bardon <i>et al.</i> (1965). Experimental points are compared to a modified theoretical curve. . . . . | 9  |
| 2  | Schematic of experimental setup. Counters C and D are above absorber, A and B are below. Absorber is described in Section 2.1. . . . .  | 9  |
| 3  | Schematic of electrical configuration. Inputs from PMTs are indicated at left, outputs to TAC appear at right. . . . .  | 10 |
| 4  | Results of TAC / MCA calibration, plus linear fit . . . . .   | 10 |
| 5  | Schematic of counter efficiency calibration . . . . .   | 11 |
| 6  | Plot of 100 sec. measurements for PMT A . . . . .   | 15 |
| 7  | Plot of 100 sec. measurements for PMT B . . . . .   | 15 |
| 8  | Plot of 100 sec. measurements for PMT C . . . . .   | 16 |
| 9  | Plot of 100 sec. measurements for PMT D . . . . .   | 16 |
| 10 | Plot of efficiencies of PMT A . . . . .   | 19 |
| 11 | Plot of efficiencies of PMT B . . . . .   | 19 |
| 12 | Plot of efficiencies of PMT C . . . . .   | 20 |
| 13 | Plot of efficiencies of PMT D . . . . .   | 20 |
| 14 | Results of experiment, with curve fit . . . . .   | 22 |

### *Abstract*

An experiment is designed to measure the lifetime of the cosmic muon. The photo-multiplier tubes and electronics used in the experiment are characterized and parameters are optimized for maximum efficiency. The observed lifetimes are fit with a curve to determine a mean lifetime of  $2.10 \text{ uS} \pm 0.05 \text{ uS}$ .

# 1 Introduction

Philosophers in Ancient Greece took their part in the study of particle metaphysics by postulating the existence of matter in discrete, irreducible quanta they called “atoms.” Many centuries later, physicists discovered the constituents of atoms, known as subatomic particles. The overwhelming body of experimental evidence available today tells us that all matter is composed of three fundamental particles: the proton, neutron and electron.

What makes these three particles special? The proton, neutron and electron are the most stable particles observed by man. Physicists have discovered dozens upon dozens of “new” particles since the advent of the particle accelerator. These new particles require great amounts of energy to produce, and even then they only last for a tiny fraction of a second (on the order of  $10^{-10}$  seconds) before decaying. In comparison, the electron has a lifetime of *at least*  $10^{26}$  years! [1]

In this experiment we make use of astrophysical particle accelerators to study a short-lived relative of the electron: the muon. When high-energy particles from outer space collide with the Earth’s upper atmosphere, various exotic particles are produced that decay quickly. Muons are a common by-product of these decays, and some muons are given enough kinetic energy to travel to the Earth’s surface before they decay.

Upon the decay of a muon, an electron is emitted in its place, often with sufficient kinetic energy to send it through several meters of air (or a decimeter of most dense materials) before stopping. Our experiment aims to “capture” cosmic muons and time the emission of the resultant electron. Many muon decays must be observed to make a statistically significant measurement of mean lifetime.

## 2 Experimental Apparatus

An individual particle can not provide enough stimulus to elicit a reaction from any human sense, so indirect methods must be used to study fundamental particles. Some indirect methods, including those used since the early 1900’s [2], employ a target, barrier or absorber with which the particle(s) will interact. Those interactions are then studied to uncover fundamental truths about the particle(s) under study.

### 2.1 Absorber

To capture a cosmic muon we need to absorb its kinetic energy such that it slows to a stop inside our experiment. We choose our absorber material for its electron density (or small nuclei / low  $Z$ ), as muons passing through this material will interact primarily with atomic electrons[1]. In these interactions the atoms become excited or ionized, and the muon loses some energy as a result. We design the absorber to be large enough to stop cosmic muons, but not so large that we also stop the decay electrons from escaping!

The Bethe-Bloch equation gives the mean rate of energy loss (or stopping power) in matter as a function of many variables including the atomic number of the matter and the incident particle’s charge and speed. To summarize this equation and the units which we

will see in our data:

$$-\frac{dE}{dx} \propto Kz^2 \frac{Z}{A} \frac{1}{\beta^2} \quad (1)$$

$$\left[ -\frac{dE}{dx} \right] = \left[ \frac{\text{MeV} \cdot \text{cm}^2}{\text{g}} \right] \quad (2)$$

We use predetermined results from this equation for our experiment, but what we take from it is the relationship between material density, particle speed and stopping power. From the spectrum of decay electron momenta (see Figure 1 [4]) we determined the absorber should be about 60 MeV “in diameter.” That is, an electron emitted in the center of the absorber should not lose more than 30 MeV before escaping.

We used a rough estimate of the stopping power of  $2.2\text{MeVcm}^2\text{gm}^{-1}$  and assumed a specific gravity of unity [3] to determine our radius:  $60\text{MeV}/(1.00\text{gcm}^3 \cdot 2.2\text{MeVcm}^2\text{g}^{-1}) = 27\text{cm}$ . Finally, we constructed a 29.5 cm H x 28 cm W x 62 cm L absorber by stacking books upon each other.

## 2.2 Counters

Immediately surrounding our absorber are four “counters,” each comprised of a plastic scintillator optically joined to a photo-multiplier tube and wrapped in thin, opaque material. The counter’s job is to signal when a charged particle passes through the scintillator. The actual signal coming from the counter is a small “tail pulse,” typically -100 mV in amplitude (all signals are negative) and a few 10s of nanoseconds in duration. To distinguish the counters used in our experiment, we have labelled them with the Roman letters A, B, C and D.

As in our absorber, cosmic muons (and electrons) will pass through each scintillator, exciting some of the atoms in the plastic. As these atoms relax, they will emit optical photons; the scintillators in our experiment will yield a few hundred photons in response to a typical particle event. Through total internal reflection, the photons eventually make it to one “end” of the scintillator, where they can be detected. The scintillators cover a horizontal area of about 60 x 25 cm and are 1 cm thick. Two scintillators were used on either side of the absorber; see Figure 2 for a schematic of our setup.

A photo-multiplier tube (PMT) is employed to detect the photons emitted within the scintillator. The PMT relies on the photoelectric effect and a strong electric field to produce accelerated electrons from the few incoming photons. Multiple dynodes held at increasing potentials create a cascade effect, amplifying the number of particles incident on the PMT. The electrons are collected at an anode at the rear of the PMT, and are presented through a BNC connector on the PMT base. A high-voltage power supply is used to bias each PMT; the tubes require up to 2000V of bias power but consume very little current (about 1 mA).

## 2.3 Electronic modules

The signals coming from the PMTs vary in height and width, depending on the amount of energy deposited in the scintillator. Note the scintillator does not care about the charge or the mass of the particle, it only responds to energy deposition (formally,  $dE/dX$ , as in

Equation 1). In addition to particle signals, the output from the PMT includes several types of electrical noise.

Specialized electronic modules must be used to extract valid signals from noise and background events. The actual electronic modules used are known as NIM modules (Nuclear Instrumentation Methods), and a “NIM crate” is provided to power these modules. The modules are compact and reconfigurable within the crate; they are joined by various lengths of cabling with quick-release “LEMO” style connectors. Signal propagation times within these cables have been measured and their approximate values (typ. 2, 4, 8) in nanoseconds are marked on the insulation of each cable.

### 2.3.1 Discriminator

We used a LeCroy Quad Discriminator (Model 821), containing four discriminator circuits. A discriminator inputs PMT signals and outputs a well-defined pulse for selected inputs. Each discriminator has an adjustable threshold which may be set from -30 mV to about -2 V. Input signals that swing below the threshold trigger an output pulse, -800 mV in amplitude and 50 nS in width (known as a NIM pulse). Discriminators are used to “ignore” noise signals while passing particle signals.

### 2.3.2 Logic

We stacked two counters on each other to acquire “coincidence” signals (see Figure 2). Random fluctuations of noise in a PMT can trigger a discriminator, producing a false event. To avoid measuring false events, we required signals from two adjacent counters that were coincident in time. For such a requirement we used the LeCroy 4-fold Logic Unit (model 365AL). This module outputs a NIM pulse when a selected number of coincident NIM pulses (also known as a “coincidence level”) appear at any of the four inputs. The output pulse can be suppressed by a “veto” signal, also a NIM logic input.

If the coincidence level is set to one, the logic unit acts as an OR gate, producing an output when any input is activated (and the “veto” signal is not present, assume this from now on). We connected two adjacent counters to a logic unit with a coincidence level of two to produce coincidence signals; this configuration was an effective AND gate. Both OR and AND gates appeared in our experimental setup, see Figure 3. It should be noted that the logic unit added a 10 nS delay between input and output.

### 2.3.3 Gate generator

We used two Joerger model GG gate generators in two different roles in this experiment. In theory, a gate generator acts much like a discriminator, outputting a NIM pulse with a preselected width immediately upon receiving an input pulse. With some additional outputs, the gate generator can also act like a delay line, outputting a pulse at some predefined interval after the input pulse.

The gate generator was used to define the window of time in which we look for muon decay events. Events from high-energy muons that pass through the experiment without decaying created two coincidence signals in a very short interval. A 100 nS delay was incorporated to ignore these events. A 10 uS gate was connected after the delay to define

the ceiling for lifetime measurements. This setup is described in more detail below (see Section 3.3).

#### 2.3.4 Time to amplitude converter

A Time to Amplitude Converter (TAC) module was used to convert lifetime measurements into analog voltages. This conversion enables slower data acquisition (DAQ) systems to capture relatively quick timing signals. The conversion is accomplished through two NIM logic inputs: “start” and “stop”. The time between a start signal and a stop signal is measured, then a fixed-width positive square pulse is output with an amplitude proportional to the measured time.

The module contains some logic to avoid improper measurements: sequential start pulses caused previous starts to be invalidated, and stops that appeared after the window of measurement (10uS) were ignored. This module also contains scaling controls to allow a range of measurements. We set the “Range” control to 100 nS and the “Mult[plier]” control to 100, for an effective measurement range of  $100\text{nS} \times 100 = 10\text{uS}$ . The output of the TAC was connected directly to our DAQ system with a 2 m BNC cable.

### 2.4 Data acquisition system

A computer with a Multi-Channel Analyzer (MCA) card was used to record the signals output by the TAC. The height of each input pulse was analyzed and stored as a count in one of 2048 bins; each bin represented a range of input pulses  $\sim 5$  mV wide. The bin range was set within the software; for our experiment the “ADC Gain” was set to 2048. The raw data (counts in each bin) from our experiment was saved in a text file that was later analyzed with statistical software including Gnuplot and ROOT.

### 2.5 Other equipment

Common lab equipment was used to aid the configuration of our experiment. We used a Tektronix TDS 380 Digital Oscilloscope to view signals from the PMT and calibrate our NIM pulse widths (from discriminators, gates, etc.). A Keithley bench-top DMM is used to measure discriminator thresholds. A HP 5134 universal counter is used to make estimates of noise and signal rates, while a Jorway Model 1880B BCD scaler was employed when exact counts were required.

## 3 Procedure

Before our apparatus can be used to extract meaningful and accurate results, we had to characterize and configure several pieces of equipment. We needed to ensure the PMTs were biased with the proper voltage and were outputting valid and measurable signals. The discriminator thresholds were carefully selected to provide a minimum noise margin and avoid ignoring valid signals. We also had to fully understand the signals entering and exiting the TAC and how they were represented by the MCA software.

### 3.1 Calibration

To determine the physical meaning behind the output from the MCA software, we simulated decay events and recorded a small amount of data. A tail pulse generator (BNC model BH-1) with an adjustable delay was connected to the TAC inputs, and the MCA software collected the resulting signals. We used our oscilloscope to verify the time between the start and stop signals we generated, then we recorded the MCA bin in which these signals appeared.

It should be noted that this procedure was a simultaneous calibration of the TAC and the MCA hardware. Since these two individual pieces of hardware exhibit very linear responses to their inputs, we feel no “intermediate” calibration was required. As such, the MCA output can be interpreted as time signals, with each count representing one decay measurement.

### 3.2 Counter characterization

Our next step was to bias each PMT with the optimum voltage to achieve a good signal to noise ratio. Using several discriminators, a gate generator and several scalers, we counted cosmic rays for 100 seconds at three arbitrarily chosen thresholds (-30, -60 and -90 mV). This exercise was repeated for a range of bias voltages, using each counter (one at a time). The goal of this exercise is to find a range of bias voltages across which the count rate does not change appreciably. This would appear as a “plateau” in a graph of counts vs. bias voltage, often referred to as a “plateau curve.” The plateau voltage is the point at which we have achieved an optimum signal to noise ratio; this voltage was used to bias the PMT for the remainder of the experiment.

We then determined the correct discriminator threshold by measuring the counters’ efficiencies at various thresholds. This determination was made by counting coincidence signals (generated by various cosmic rays) in a “3-2” setup: three counters arranged such that the top and bottom counters overlap each other in an area equal to the width of the counter placed in the middle. See Figure 5 for a schematic of this setup. The counters are connected to discriminators set to fairly low thresholds for this exercise. In this configuration, we can detect when the middle counter (a.k.a. the Counter Under Test, CUT) *should* produce a signal. The assumption is: if we receive coincident signals from the top and bottom counters, there most likely was a particle passing through the overlapping area, and therefore we should see a coincident signal from the CUT.

Using logic units, we produced outputs for double (top and bottom) and triple signal coincidences, and then we counted these signals until we achieved at least 1000 double coincidences. The counts are compared as such: triple coincidences / double coincidences = CUT efficiency (in %). This procedure began with the CUT threshold at its lowest setting ( $\sim -30$  mV) and was repeated with increasing thresholds until we saw 20% efficiency or less. The “correct” threshold is chosen just above the “knee” in a graph of efficiency vs. threshold (see Figure 10 for an example). We chose this value to ensure maximum particle detection efficiency with the least amount of false triggers from noise.

After the counters and discriminators are set up, we had to do a quick check of counter signal rates (or “trigger rates”) to ensure our equipment was behaving as expected. To ensure a counter is not too noisy to provide reliable results, we verify its trigger rate is under 100 Hz. We then set the counters up for the experiment, as in Figure 2, and check the double coincidence rates in the top and bottom pairs of counters.

### 3.3 Logic setup

In most particle physics experiments, logic is used as a first-order filter to select events of interest and reject background events. Figure 3 contains a schematic of the logic used in our experiment. Each counter's signal was run through a discriminator before arriving at a logic unit. We used double-coincidence signals as triggers, so an "AND" logic configuration is used for the top and bottom pairs of counters. The top pair produced the TAC start signal for our experiment, while either the top or bottom pair could produce the TAC stop signal. This required the use of an "OR" logic unit.

We used the veto feature of the OR logic unit to prevent a TAC stop signal from appearing too early or too late. The 100 nS delay held the veto signal high (preventing output) to ignore non-decay events, while the 10 uS gate held the veto signal low (allowing output) to accept signals within our window of measurement. To ensure accurate timing, we used various lengths of cabling in our setup to ensure start and stop signals travelled through the same "electrical length," that is, signals coming from any counter reach the TAC stop input in the same amount of time required to reach the TAC start input.

### 3.4 Measurement

Once the equipment was characterized and configured, the experiment practically ran itself. No further human intervention was required until it was time to turn the equipment off! The data acquisition system ran continuously throughout the experiment, recording events as they occurred. We "eyeballed" the data once a day throughout the experiment to make sure we collected no unintentional results (i.e. spurious peaks in the histogram). When we were satisfied with the number of events we had collected (our minimum requirement was 10,000 events), we terminated the experiment and saved our results for off-line analysis.

## 4 Results

### 4.1 Calibration

Our raw data is presented in Table 1 and Figure 4. Using Gnuplot we fitted a line to our data to interpolate measurements between the points we recorded. The parameters of our fit are summarized in Table 2.

### 4.2 Counter characterization

The raw data from our bias voltage exercises are presented in Tables 3, 4, 5 and 6. Finding the plateau in these data was rather difficult, so we used an analytical approach. We produced "derivative" plots by graphing the difference between two measurements: see Figures 6, 7, 8 and 9. We looked for a coincident "dip" in these plots, a bias voltage around which the curves took on a local minimum. This corresponded to the plateau voltage for a particular PMT.

The raw data from our counter efficiency measurements are presented in Tables 7, 8, 9 and 10. These data are plotted in Figures 10, 11, 12 and 13. We choose the "knee" point of these curves by inspection of the plots. Our choices of bias voltages and discriminator

thresholds are summarized in Table 11. Our check of single and double coincidence rates are summarized in Table 12.

### 4.3 Measurement

The MCA software output contained decay counts in 2048 bins. To reduce the error in each bin we used ROOT to re-bin the data into 30 bins; these results are displayed in Table 13. The re-binned histogram with a curve fit is shown in Figure 14.

## 5 Analysis and Interpretation

### 5.1 Theory

Once our experiment was configured (as described in Section 3) we did a quick check of coincidence rates. Empirical data from horizontal detector based experiments yields a  $\sim 1$  GeV muon intensity at sea level of about 1 count /  $\text{cm}^2 \cdot \text{min}$ . With this intensity, our 60 x 25 cm detectors (1500  $\text{cm}^2$ ) should give a signal rate of 25 Hz. Our observed double coincidence rates agreed with this result very well, so we agreed our experiment was in fact properly configured.

Given the single counter rates we calculated the rate of accidental double coincidences caused by the overlapping of two noise signals:  $r_{acc} = N_1 \cdot N_2 \cdot 2 \cdot \tau$  where  $N_1$  and  $N_2$  are the single rates and  $\tau$  is the pulse width. For our measured single rates, we saw a maximum accidental rate of 35 Hz  $\cdot$  100 Hz  $\cdot$  2  $\cdot$  50 nS = 3.5 mHz (that's milliHertz!). The rate of accidental events (two accidental double coincidences within 10  $\mu\text{S}$ ) was calculated in a similar fashion, and was determined to be 5.28 mHz. This rate was well below the muon flux through our detectors; the accidental background was not significant enough to cause any worry.

### 5.2 Experiment

The data from our experiment followed the statistical law of radioactivity. To find the mean lifetime from our data, we fit a modified decay equation (see Equation 3) to our histogram. We included a constant term  $B$  to account for our accidental background, since it is equally probable that an accidental event would appear in any bin. Note that  $N_0$  represents the number of counts in bin zero.

$$N = N_0 e^{-\frac{t}{\tau}} + B \tag{3}$$

ROOT was used to perform the fit, see the results in Table 14. ROOT uses a weighted sum-of-squares algorithm to make its fit. ROOT also propagated errors through its fit, using  $\sqrt{n}$  as the default error on each bin. We neglected the errors from our linear interpolations of TAC and MCA measurements due to the relatively low error in the slope parameter. In re-binning the MCA output, we eliminate most uncertainties in the x-axis (bin number), so the  $\sim 50\%$  error in the intercept parameter is inconsequential.

ROOT also produced a chi-square value to describe its fit. In choosing the number of bins with which to re-bin our original data, we used the value  $\chi^2/\nu$  from fits of many

different binning scenarios (from 10 to 100 bins) to select our final result of 30 bins. Our result of  $\chi^2/\nu = 1.03$  gives us no reason to believe ROOT's fit does not describe our data.

## 6 Conclusion

This lab was an excellent introduction to experimental particle physics. The painful amount of data taking and re-taking during counter characterization yielded an intimate knowledge of the workings of these measurement devices, which will prove useful in future experiments involving particle detection. The process of waiting for our data was equally tense and exciting, and our final result was quite satisfactory. The latest issue of Physics Letters (see Reference [1]) lists the muon lifetime at 2.197  $\mu\text{S}$ ; our result is only 4.3% below the agreed lifetime!

## 7 Tables and Figures

| Pulse Delay<br>( $\mu\text{S}$ ) | MCA Bin |
|----------------------------------|---------|
| 0.50                             | 104     |
| 0.75                             | 155     |
| 1.00                             | 207     |
| 1.25                             | 258     |
| 1.50                             | 309     |
| 1.75                             | 361     |
| 2.00                             | 412     |
| 2.50                             | 513     |
| 3.00                             | 615     |
| 3.50                             | 721     |
| 4.00                             | 822     |
| 5.00                             | 1028    |
| 6.00                             | 1234    |
| 8.00                             | 1645    |

Table 1: Results of TAC / MCA calibration

| Parameter | Value    | Error<br>+/- | Error<br>% |
|-----------|----------|--------------|------------|
| Slope     | 205.456  | 0.1173       | 0.0571     |
| Intercept | 0.834415 | 0.422        | 50.58      |

Table 2: Details of linear fit

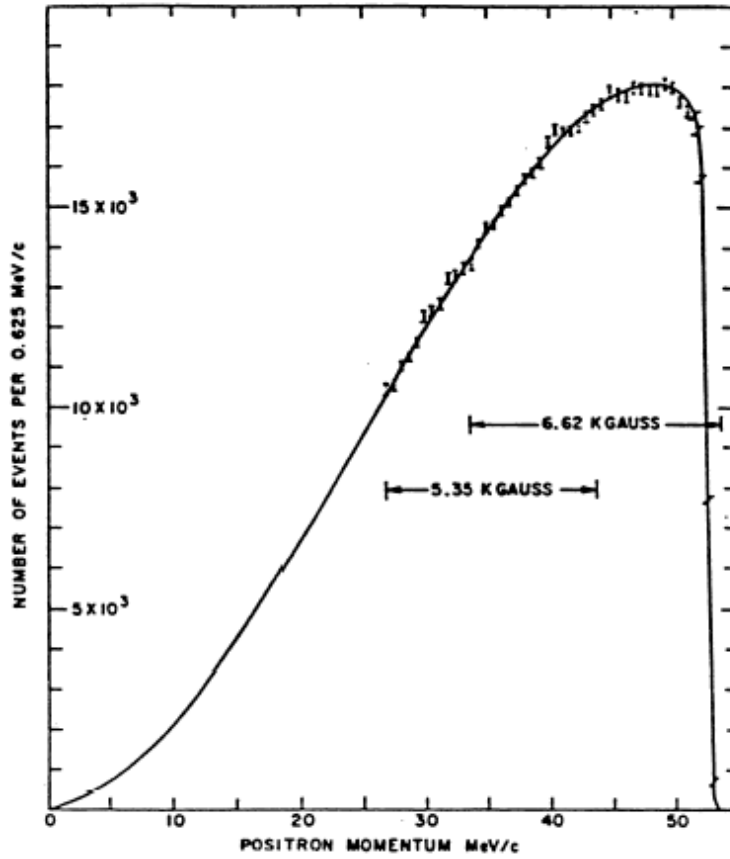


Figure 1: The distribution of electron kinetic energies in muon decay at rest. Data from the experiment of Bardon *et al.* (1965). Experimental points are compared to a modified theoretical curve.

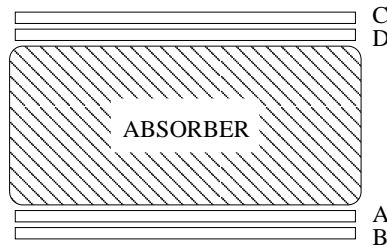


Figure 2: Schematic of experimental setup. Counters C and D are above absorber, A and B are below. Absorber is described in Section 2.1.

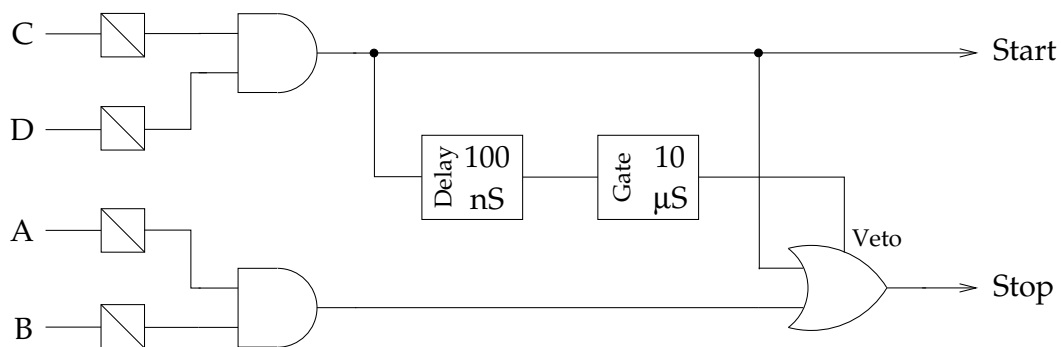


Figure 3: Schematic of electrical configuration. Inputs from PMTs are indicated at left, outputs to TAC appear at right.

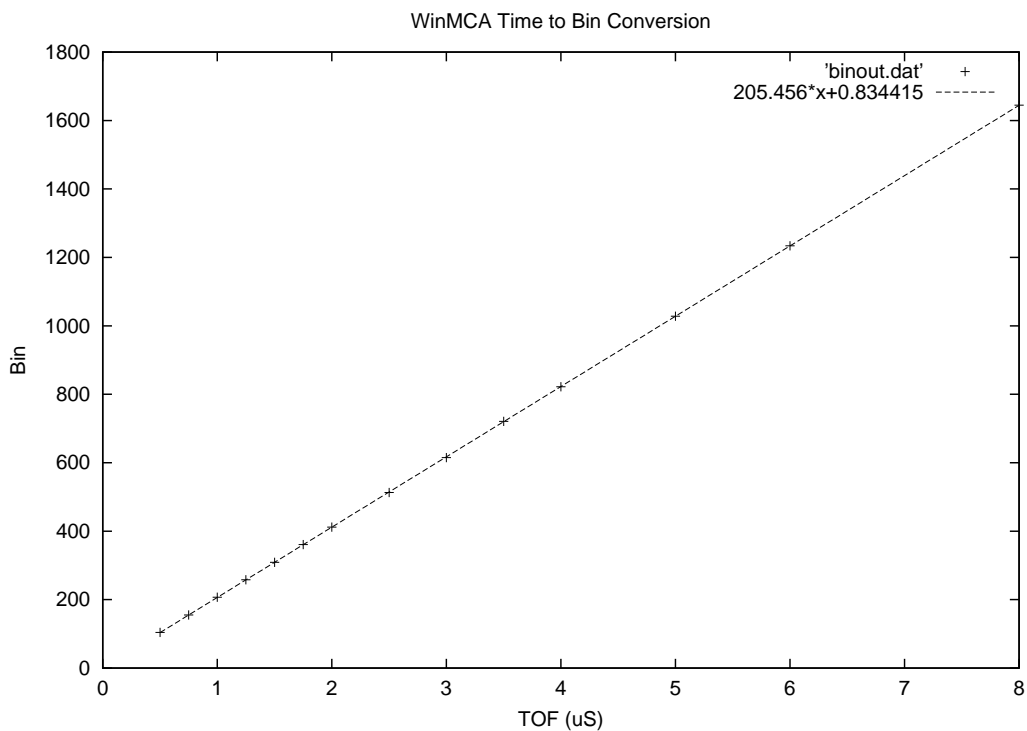


Figure 4: Results of TAC / MCA calibration, plus linear fit

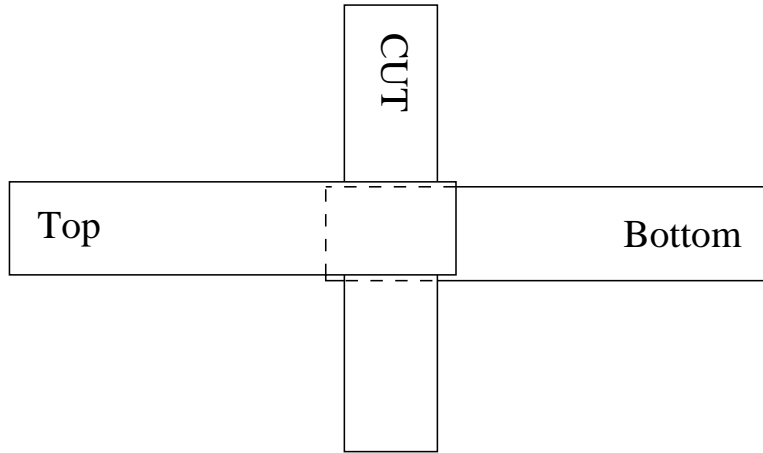


Figure 5: Schematic of counter efficiency calibration

| Bias Voltage (V) | -30 mV Counts | -60 mV Counts | -90 mV Counts |
|------------------|---------------|---------------|---------------|
| 1200             | 32            | 0             | 0             |
| 1225             | 48            | 5             | 0             |
| 1250             | 92            | 7             | 1             |
| 1275             | 160           | 11            | 5             |
| 1300             | 264           | 24            | 10            |
| 1325             | 471           | 58            | 13            |
| 1350             | 659           | 97            | 35            |
| 1375             | 1009          | 189           | 53            |
| 1400             | 1324          | 316           | 106           |
| 1425             | 1772          | 411           | 163           |
| 1450             | 2189          | 672           | 243           |
| 1475             | 2853          | 957           | 400           |
| 1500             | 3699          | 1247          | 576           |
| 1525             | 4785          | 1552          | 826           |
| 1550             | 6382          | 1951          | 1068          |
| 1575             | 7116          | 2418          | 1437          |
| 1600             | 8363          | 3065          | 1759          |
| 1625             | 9839          | 3904          | 2220          |
| 1650             | 12643         | 5090          | 2339          |
| 1675             | 13953         | 6240          | 3467          |
| 1700             | 16834         | 7163          | 4099          |
| 1725             | 20157         | 8534          | 5147          |
| 1750             | 22613         | 10025         | 6252          |
| 1775             | 28725         | 12112         | 7418          |
| 1800             | 30455         | 14625         | 8619          |

Table 3: Results of 100 sec. of measurement with PMT A at three thresholds

| Bias Voltage<br>(V) | -30 mV Counts | -60 mV Counts | -90 mV Counts |
|---------------------|---------------|---------------|---------------|
| 1200                | 82            | 8             | 3             |
| 1225                | 115           | 13            | 2             |
| 1250                | 254           | 26            | 13            |
| 1275                | 430           | 49            | 7             |
| 1300                | 739           | 85            | 22            |
| 1325                | 1160          | 163           | 46            |
| 1350                | 1683          | 283           | 84            |
| 1375                | 2147          | 514           | 175           |
| 1400                | 3056          | 841           | 297           |
| 1425                | 4059          | 1207          | 387           |
| 1450                | 5920          | 1669          | 602           |
| 1475                | 7664          | 2278          | 965           |
| 1500                | 11757         | 3168          | 1324          |
| 1525                | 14254         | 4551          | 1855          |
| 1550                | 22916         | 6723          | 2361          |
| 1575                | 34139         | 10125         | 3694          |
| 1600                | 54597         | 14468         | 5897          |
| 1625                | 91058         | 19340         | 8131          |
| 1650                | 167114        | 26206         | 10643         |
| 1675                | 208546        | 34756         | 15214         |
| 1700                | 274816        | 50375         | 20066         |
| 1725                | 351244        | 77343         | 26795         |
| 1750                | 440048        | 120388        | 36269         |
| 1775                | 509062        | 169676        | 51581         |
| 1800                | 588584        | 245054        | 83480         |

Table 4: Results of 100 sec. of measurement with PMT B at three thresholds

| Bias Voltage<br>(V) | -30 mV Counts | -60 mV Counts | -90 mV Counts |
|---------------------|---------------|---------------|---------------|
| 1200                | 1             | 0             | 0             |
| 1225                | 2             | 0             | 0             |
| 1250                | 4             | 0             | 0             |
| 1275                | 13            | 2             | 0             |
| 1300                | 20            | 1             | 0             |
| 1325                | 38            | 1             | 0             |
| 1350                | 67            | 7             | 2             |
| 1375                | 107           | 11            | 2             |
| 1400                | 235           | 21            | 7             |
| 1425                | 426           | 33            | 10            |
| 1450                | 669           | 56            | 10            |
| 1475                | 979           | 87            | 20            |
| 1500                | 1327          | 171           | 44            |
| 1525                | 1800          | 279           | 69            |
| 1550                | 1982          | 430           | 122           |
| 1575                | 2423          | 663           | 191           |
| 1600                | 3055          | 937           | 350           |
| 1625                | 4308          | 1288          | 511           |
| 1650                | 7041          | 1659          | 831           |
| 1675                | 12919         | 1753          | 988           |
| 1700                | 34102         | 2316          | 1479          |
| 1725                | 69901         | 2841          | 1845          |
| 1750                | 133131        | 3793          | 1995          |
| 1775                | 213290        | 6294          | 2353          |
| 1800                | 264180        | 17858         | 2947          |

Table 5: Results of 100 sec. of measurement with PMT C at three thresholds

| Bias Voltage<br>(V) | -30 mV Counts | -60 mV Counts | -90 mV Counts |
|---------------------|---------------|---------------|---------------|
| 1200                | 0             | 0             | 0             |
| 1225                | 0             | 0             | 0             |
| 1250                | 0             | 0             | 0             |
| 1275                | 0             | 0             | 0             |
| 1300                | 2             | 1             | 0             |
| 1325                | 1             | 0             | 0             |
| 1350                | 1             | 0             | 0             |
| 1375                | 3             | 0             | 0             |
| 1400                | 6             | 1             | 0             |
| 1425                | 13            | 1             | 0             |
| 1450                | 25            | 1             | 0             |
| 1475                | 53            | 5             | 0             |
| 1500                | 80            | 8             | 2             |
| 1525                | 125           | 11            | 1             |
| 1550                | 232           | 14            | 6             |
| 1575                | 373           | 30            | 10            |
| 1600                | 565           | 59            | 12            |
| 1625                | 782           | 91            | 29            |
| 1650                | 1071          | 132           | 42            |
| 1675                | 1166          | 221           | 53            |
| 1700                | 1617          | 344           | 118           |
| 1725                | 1952          | 543           | 161           |
| 1750                | 2476          | 768           | 210           |
| 1775                | 3265          | 969           | 381           |
| 1800                | 3794          | 1223          | 524           |
| 1825                | 4650          | 1441          | 733           |
| 1850                | 5463          | 1661          | 1014          |
| 1875                | 6214          | 2074          | 1265          |
| 1900                | 7242          | 2668          | 1498          |

Table 6: Results of 100 sec. of measurement with PMT D at three thresholds

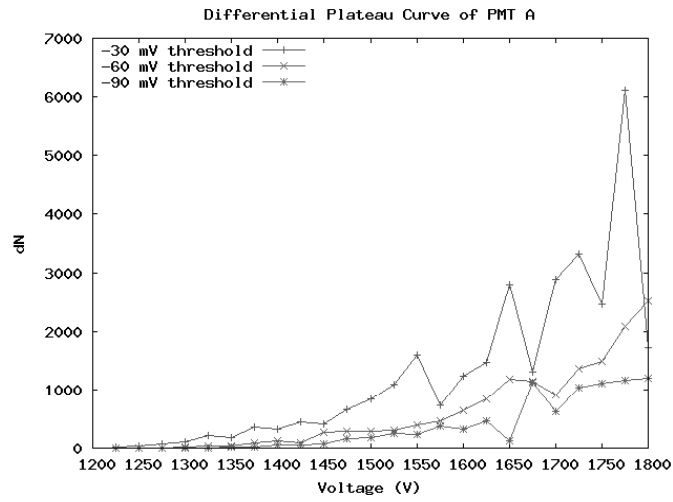


Figure 6: Plot of 100 sec. measurements for PMT A

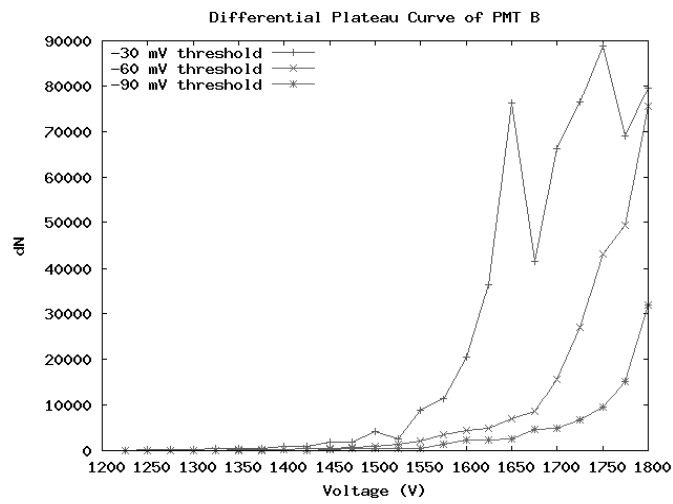


Figure 7: Plot of 100 sec. measurements for PMT B

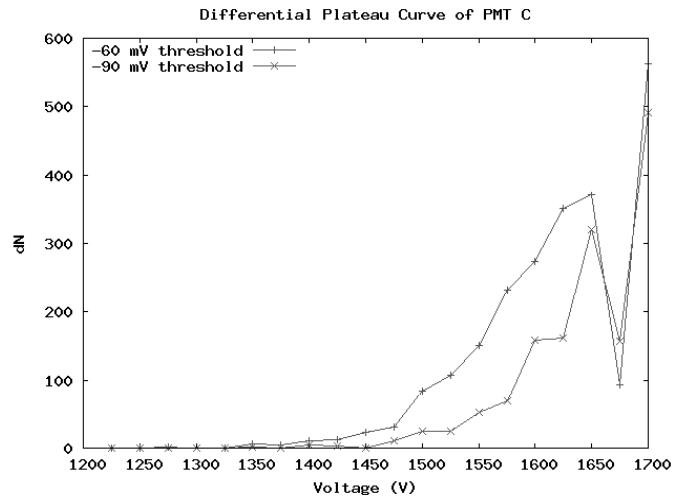


Figure 8: Plot of 100 sec. measurements for PMT C

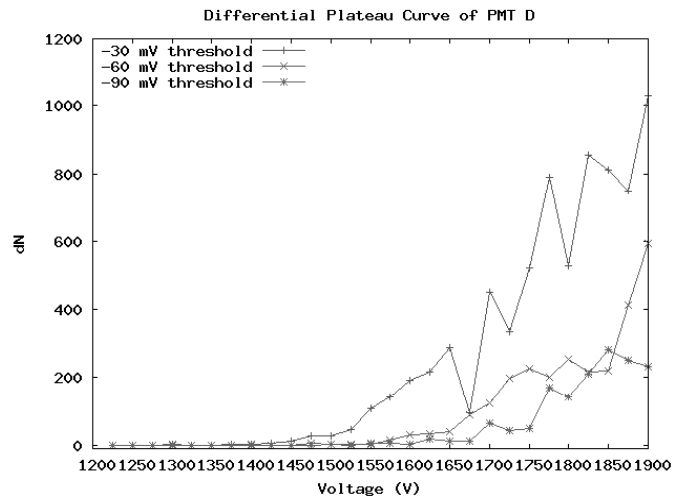


Figure 9: Plot of 100 sec. measurements for PMT D

| Threshold<br>(mV) | Triple coinc.<br>count | Double coinc.<br>count | Ratio<br>3 / 2 |
|-------------------|------------------------|------------------------|----------------|
| 50                | 911                    | 1000                   | 0.911          |
| 75                | 910                    | 1000                   | 0.910          |
| 100               | 897                    | 1002                   | 0.895          |
| 125               | 891                    | 1000                   | 0.891          |
| 150               | 833                    | 1000                   | 0.833          |
| 175               | 756                    | 1001                   | 0.755          |
| 200               | 699                    | 1106                   | 0.632          |
| 225               | 502                    | 1004                   | 0.500          |
| 250               | 370                    | 1000                   | 0.370          |
| 275               | 259                    | 1001                   | 0.259          |
| 300               | 247                    | 1000                   | 0.247          |

Table 7: Efficiency measurements for counter A

| Threshold<br>(mV) | Triple coinc.<br>count | Double coinc.<br>count | Ratio<br>3 / 2 |
|-------------------|------------------------|------------------------|----------------|
| 50                | 946                    | 1002                   | 0.944          |
| 75                | 931                    | 1003                   | 0.928          |
| 100               | 933                    | 1001                   | 0.932          |
| 125               | 930                    | 1002                   | 0.928          |
| 150               | 917                    | 1001                   | 0.916          |
| 175               | 870                    | 1004                   | 0.867          |
| 200               | 820                    | 995                    | 0.824          |
| 225               | 757                    | 1004                   | 0.754          |
| 250               | 687                    | 1006                   | 0.683          |
| 275               | 566                    | 1001                   | 0.565          |
| 300               | 491                    | 1006                   | 0.488          |

Table 8: Efficiency measurements for counter B

| Threshold<br>(mV) | Triple coinc.<br>count | Double coinc.<br>count | Ratio<br>3 / 2 |
|-------------------|------------------------|------------------------|----------------|
| 50                | 966                    | 1002                   | 0.964          |
| 75                | 947                    | 1003                   | 0.944          |
| 100               | 860                    | 1001                   | 0.859          |
| 125               | 630                    | 1002                   | 0.629          |
| 150               | 441                    | 1002                   | 0.440          |
| 175               | 283                    | 1003                   | 0.282          |
| 200               | 199                    | 1004                   | 0.198          |

Table 9: Efficiency measurements for counter C

| Threshold<br>(mV) | Triple coinc.<br>count | Double coinc.<br>count | Ratio<br>3 / 2 |
|-------------------|------------------------|------------------------|----------------|
| 50                | 913                    | 1002                   | 0.911          |
| 75                | 636                    | 1001                   | 0.635          |
| 100               | 332                    | 1004                   | 0.331          |
| 125               | 188                    | 1005                   | 0.187          |
| 150               | 104                    | 1011                   | 0.103          |
| 175               | 64                     | 1003                   | 0.064          |
| 200               | 53                     | 1001                   | 0.053          |

Table 10: Efficiency measurements for counter D

| Counter | Bias Voltage<br>(V) | Threshold<br>(mV) |
|---------|---------------------|-------------------|
| A       | 1700                | -110              |
| B       | 1675                | -135              |
| C       | 1675                | -60               |
| D       | 1725                | -30               |

Table 11: Operating parameters for counters

| Coinc. | Counter(s) | Rate<br>(Hz) |
|--------|------------|--------------|
| Single | A          | 35           |
| Single | B          | 100          |
| Single | C          | 50           |
| Single | D          | 35           |
| Double | A+B        | 22           |
| Double | C+D        | 24           |

Table 12: Coincidence rates from counters in experimental configuration

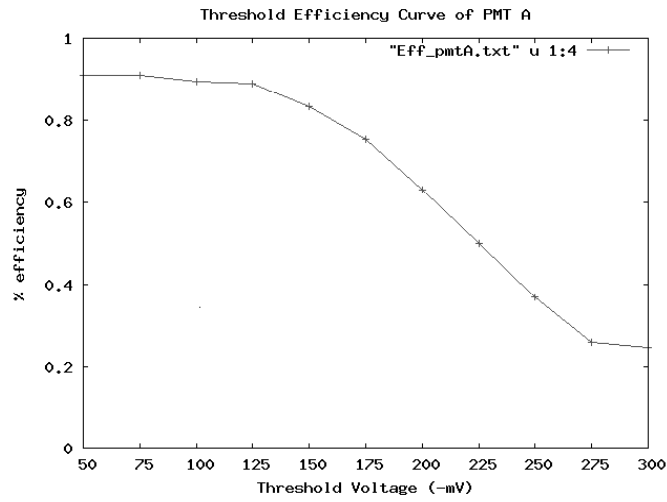


Figure 10: Plot of efficiencies of PMT A

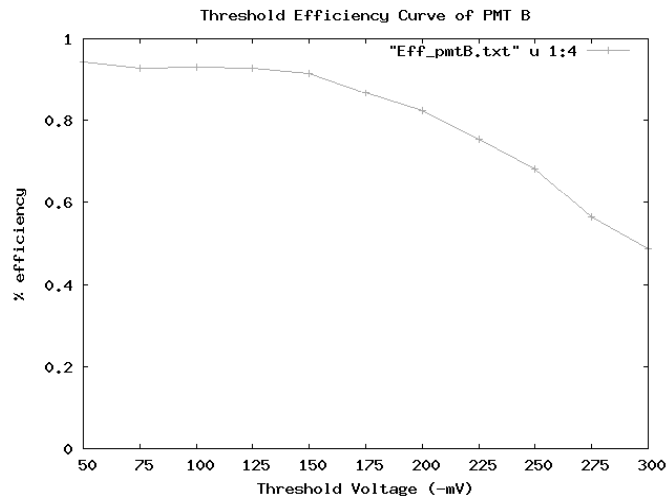


Figure 11: Plot of efficiencies of PMT B

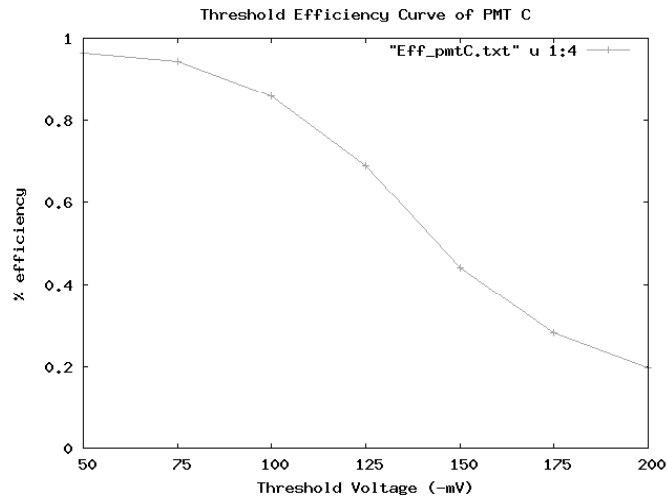


Figure 12: Plot of efficiencies of PMT C

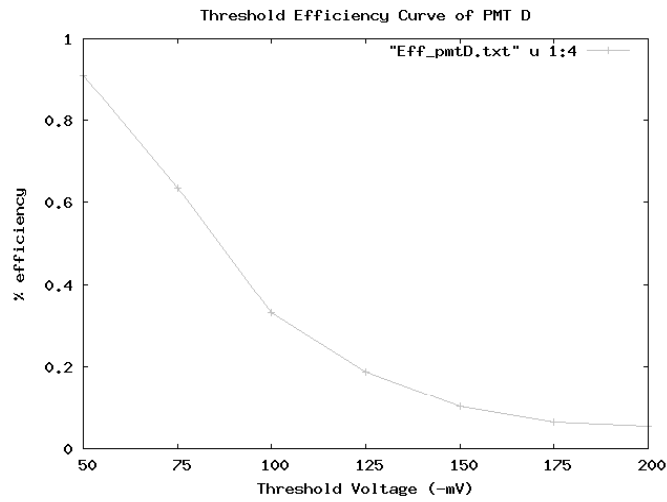


Figure 13: Plot of efficiencies of PMT D

| Bin | Time<br>( $\mu\text{S}$ ) | Counts |
|-----|---------------------------|--------|
| 1   | 0.76                      | 1171   |
| 2   | 1.07                      | 1022   |
| 3   | 1.38                      | 874    |
| 4   | 1.70                      | 773    |
| 5   | 2.01                      | 654    |
| 6   | 2.32                      | 551    |
| 7   | 2.64                      | 490    |
| 8   | 2.95                      | 431    |
| 9   | 3.26                      | 358    |
| 10  | 3.58                      | 333    |
| 11  | 3.89                      | 291    |
| 12  | 4.20                      | 217    |
| 13  | 4.52                      | 225    |
| 14  | 4.83                      | 191    |
| 15  | 5.14                      | 192    |
| 16  | 5.46                      | 135    |
| 17  | 5.77                      | 120    |
| 18  | 6.08                      | 133    |
| 19  | 6.40                      | 117    |
| 20  | 6.71                      | 104    |
| 21  | 7.02                      | 98     |
| 22  | 7.34                      | 90     |
| 23  | 7.65                      | 66     |
| 24  | 7.96                      | 77     |
| 25  | 8.28                      | 57     |
| 26  | 8.59                      | 62     |
| 27  | 8.90                      | 45     |
| 28  | 9.22                      | 51     |
| 29  | 9.53                      | 51     |
| 30  | 9.84                      | 32     |

Table 13: Re-binned results of experiment

| Parameter    | Value | Error<br>+/- | Error<br>% |
|--------------|-------|--------------|------------|
| $N_0$        | 7.40  | 0.024        | 0.3        |
| $\tau$       | 2.10  | 0.05         | 2.5        |
| $B$          | 28.5  | 3.9          | 13.6       |
| $\chi^2$     | 27.9  |              |            |
| $\nu$        | 27    |              |            |
| $\chi^2/\nu$ | 1.03  |              |            |

Table 14: Details of curve fit

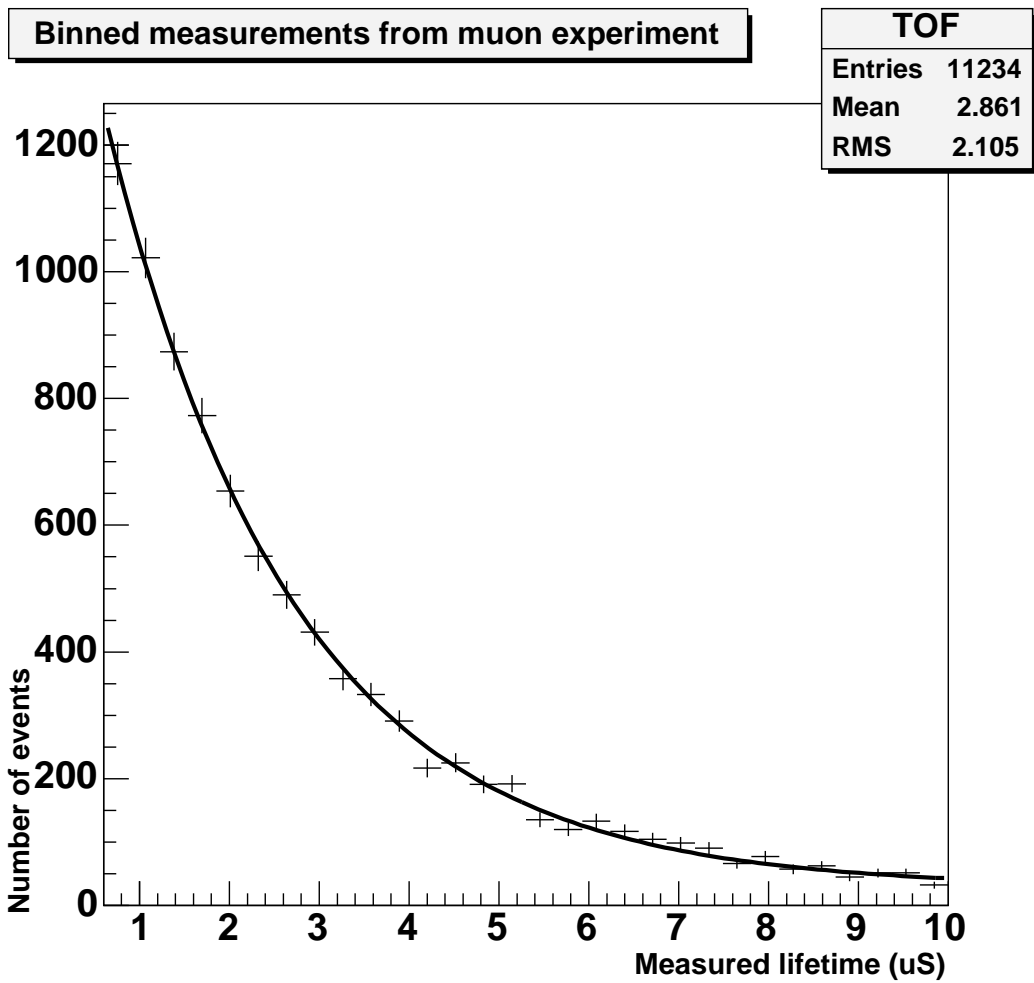


Figure 14: Results of experiment, with curve fit

## Acknowledgments

My highest praises go to Dave Dorfan for teaching physics like no other professor on the planet. His instruction through this experiment has been insightful, compelling and entertaining, to say the least. Many kudos go to Fred Kuttner for making our lab experience pleasant and free of hassle. Thanks to my partner John Wray for contributing his analytical and experimental skills to this project.

## References

- [1] S. Eidelman *et al*, Phys. Lett. B **592**, 1 (2004)
- [2] P. Tipler and R. Llewellyn, *Modern Physics*, 3rd ed. New York: W. H. Freeman and Co., 1999.
- [3] D. Dorfan, “Notes for the Muon Lifetime Experiment” handout. University of California at Santa Cruz: 2004.
- [4] R. Schumacher and R. Edelman, “Cosmic Ray Muons” handout. Carnegie Mellon University: 2002.